IEEE Access
Multidisciplinary : Rapid Review : Open Access Journal

Received January 25, 2019, accepted February 5, 2019, date of publication February 15, 2019, date of current version March 7, 2019.

Digital Object Identifier 10.1109/ACCESS.2019.2899622

GNSS Multipath Error Modeling and Mitigation by Using Sparsity-Promoting Regularization

CHAO CHEN[1,2], GUOBIN CHANG[1,2,3], NANSHAN ZHENG[1,2], AND TIANHE XU[4]
[1]NASG Key Laboratory of Land Environment and Disaster Monitoring, China University of Mining and Technology, Xuzhou 221116, China
[2]School of Environmental Science and Spatial Informatics, China University of Mining and Technology, Xuzhou 221116, China
[3]Department of Navigation Engineering, Naval University of Engineering, Wuhan 430033, China
[4]Institute of Space Science, Shandong University, Weihai 264209, China

Corresponding author: Guobin Chang (guobinchang@hotmail.com)

This work was supported by the Outstanding Innovation Scholarship for Doctoral Candidate of "Double First Rate" Construction Disciplines of CUMT.

ABSTRACT In high-accuracy global navigation satellite system (GNSS) positioning applications, the multipath is one of the primary error sources because it is hard to parameterize. Being somewhat systematic rather than purely random, the multipath should be viewed more as a signal rather than a noise. On this basis, empirically modeling the multipath is realizable. A new sidereal filtering approach based on sparsity-promoting regularization is proposed to mitigate multipath errors for static short baseline GNSS applications. The key idea of the proposed method emphasizes the use of the L_1 norm to extract multipaths from noisy carrier phase residuals. Two regularization schemes with the first- and second-order differences are considered. For each scheme, efficient numerical algorithms are developed to find solutions by using the Thomas algorithm and the Cholesky rank-one update algorithm as the core of the iteration for the first- and second-order differences, respectively. Regularization parameters or Lagrange multipliers are optimized by using the bootstrap method. By applying the proposed multipath modeling method, the average improvement ratio of the root-mean-square values of double-difference residuals can reach approximately 66.7% compared with the result without multipath mitigation in the two different datasets. Moreover, positioning precision is improved by approximately 20.8%, 26.3%, and 37.8% in the East, North, and Up directions, respectively. Moreover, the fixed rate of ambiguities is improved by 3.7% on average under the kinematic mode.

INDEX TERMS GNSS, multipath, sidereal filtering, regularization, L_1 norm, bootstrap.

I. INTRODUCTION

Double-difference technique is commonly used in GNSS applications as it can eliminate or reduce considerable errors, such as ionospheric and tropospheric delays, satellite orbit, and clock errors, especially for short baselines. An unmodeled error remains given that poor elimination occurs in general, even with the double-difference technique. This error source is the so-called multipath, which occurs when duplicate satellite transmissions are received by an antenna, wherein one transmits along a direct path from the satellite and the others arrive at a slight delay after being reflected by nearby surfaces. Although hardware-based techniques can reduce multipath errors in the received signal, avoiding multipath errors completely is impossible for receivers regardless of the type of hardware. Multipath can be the main error source for GNSS relative positioning applications, such as structural health monitoring [1], crustal motion monitoring [2], mine deformation monitoring [3], and attitude determination [4], [5]. Based on the corresponding mechanism, multipath errors can be as high as a quarter of the signal wavelength, which is a maximum change in the range of approximately 4.8 cm for GPS L_1 signal [6]. An error of this magnitude may not be tolerable in some precision applications, such as those mentioned above.

Multipath errors show certain systematic patterns to some extent because multipath errors can be viewed more as signals rather than purely random noise. This feature makes it possible to model multipath errors. In fact, denoising is crucial in multipath modeling and many signal process methods [7], [8] can be applied in this area. However, modeling multipath mathematically is often difficult due to the complex physical

The associate editor coordinating the review of this manuscript and approving it for publication was Bora Onat.

and geometrical characteristics of the environment reflecting the GNSS signal. As a result, one has to resort to empirical modeling or constructing a model by processing the GNSS data. Two modes are possible for the obtained multipath model. The first is the post-processing mode, which uses the model to correct the measurements wherein the model is constructed. The second mode is the predicting mode, which uses the model to correct the measurements obtained in the future. The latter can be used when the systematic pattern of the multipath errors repeats itself. Multipath error modeling together with the use of the model under predicting mode is also called sidereal filtering in the community. Sidereal filtering approach can only be applicable in static positioning situations because repeatability exists only in these situations.

Considerable studies have been conducted on empirical multipath error modeling and mitigation in recent years. Constructing the model and determining the repeating period are the two crucial aspects of sidereal filtering technique, and the former is the focus of this study. Constructing a model can be performed by reconstructing a systematic multipath error signal from noisy carrier phase measurement residual, denoising must be performed in the time domain. Considerable techniques can be used, such as wavelet threshold denoising [9], [10], multi-resolution analysis [11], [12], Vondrak filtering [13], empirical mode decomposition [14], [15], and stochastic state estimation [16]. The repeating period can be obtained by determining the repeating time of multipath errors and by using the three approaches commonly presented in the literature [17]–[19]. As this topic is not the focus of this work, we simply adopt aspect repeat time adjustment (ARTA) method without detailing it any further. A recently published work is devoted to this topic wherein three methods are compared in detail through experiments [20].

Hence, sidereal filtering is not the only approach for mitigating GNSS multipath errors. The ultimate cause of multipath error repeatability is the repeatability of satellite azimuth and elevation with consideration for the antenna of the static site. Thus, modeling the multipath error as a function of satellite azimuth and elevation is necessary. Any method following this reasoning can be called modeling in the space domain, whereas sidereal filtering methods can be called time–domain modeling. Moreover, space–domain methods use techniques, such as gridding [21], [22], polynomial [23], and harmonic models [24]. Determining the repeating time is generally avoided in space–domain methods because repeating time is relatively long for some constellation satellites other than GPS, such as BDS [25]; and the long repeating time hinders sidereal filtering methods from good practicability.

As mentioned above, multipath error modeling in the framework of sidereal filtering is a denoising task, which is an important topic in signal processing and applied statistics communities. As a result, the considerable amount of studies on signal processing can be used as reference. In fact, most of the existing sidereal filtering methods can find their roots in signal processing literature. Similarly, from the viewpoint of denoising, an alternative method is proposed in our previous study for constructing a Tikhonov regularization-based GNSS multipath error model [26]. In this method, L_2 norm of the first- or second-order derivative of the variable for modeling is constrained. Accordingly, a small or smooth model or a model with a small derivative of the corresponding order is preferred. In this work, a different starting point is followed, wherein a simpler model is preferred instead of a smaller model. A simpler model, which is also called sparser model, has good generalization properties [27]. Sparsity is a crucial concept in multiple disciplines, such as statistics [28], signal processing [29], [30], machine learning [31]–[33], and compressed sensing [34]. Particularly, sparsity means that fewer nonzero parameters exist in the final model. In this work, first- or second-order derivatives (or differences in the discrete case) of the multipath error signal must increase in sparsity, wherein a model with fewer nonzero differences must be constructed. Sparsity is promoted by introducing L_1 norm regularization terms by using other sparsity-promoting methods found in the literature. First-order derivative uses the minimum total variation method for 1D problems [35]. This work can be viewed as an extension of our previous work by replacing the L_2 norm with the L_1 norm. However, we would like to emphasize that this process of replacing is not trivial as it implies a fundamental strategy shift. Moreover, this work can introduce a different sparsity viewpoint to the specific field of GNSS multipath error modeling. Our own experiment on GNSS multipath error modeling shows that L_1 norm regularization generally has a slightly better performance than its L_2 norm counterpart although a detailed comparison is not presented. Some achievements are referenced from our previous study. To be more specific, two numerically efficient algorithms, namely, the Thomas algorithm and the Cholesky rank-one update algorithm, are used as the engines of iterative algorithms to obtain the solutions. Similarly, regularization coefficients, such as Lagrange multipliers, are optimized through bootstrap technique [36].

This paper is organized as follows. Section **II** presents the methodology development, including modeling with first- and second-order derivative regularization, and determining regularization coefficients by using the bootstrap method. Section **III** discusses the test results, and the last section summarizes the findings of the paper.

II. METHODOLOGY

A. PROBLEM FORMULATION

Our multipath error modeling problem considers the residuals corresponding to different satellites separately. The measurement model for an arbitrary satellite is as follows:

$$\phi_k = m_k + \eta_k, \quad k = 1, 2, \cdots, n, \tag{1}$$

where subscript k denotes the time epoch; ϕ_k denotes the carrier phase measurement residual, which is available as observables; m_k denotes the multipath error, which is viewed as the signal for reconstruction; and η_k is the equivalent noises representing all the other unmodeled errors. The multipath error signal is extracted from the residuals by minimizing one of the two following cost functions or Lagrangian notations:

$$J_1(\{m_k\}) = \sum_{k=1}^{n} w_k(\phi_k - m_k)^2 + \lambda \sum_{k=2}^{n} |m_k - m_{k-1}|, \tag{2}$$

$$J_2(\{m_k\}) = \sum_{k=1}^{n} w_k(\phi_k - m_k)^2 + \mu \sum_{k=3}^{n} |m_k - 2m_{k-1} + m_{k-2}|, \tag{3}$$

where w_k denotes the weights determined as a function of satellite elevation. The form of Eq. (2) or (3) is only a total variation regularization problem [35] [37]. The above Lagrangian notations are presented as follows in vector/matrix form:

$$J_1(\boldsymbol{m}) = (\boldsymbol{\phi} - \boldsymbol{m})^{\mathrm{T}} \boldsymbol{W} (\boldsymbol{\phi} - \boldsymbol{m}) + \lambda |\boldsymbol{\Gamma}_1 \boldsymbol{m}|_1, \tag{4}$$

$$J_2(\boldsymbol{m}) = (\boldsymbol{\phi} - \boldsymbol{m})^{\mathrm{T}} \boldsymbol{W} (\boldsymbol{\phi} - \boldsymbol{m}) + \mu |\boldsymbol{\Gamma}_2 \boldsymbol{m}|_1, \tag{5}$$

with operators

$$\boldsymbol{\Gamma}_1 = \begin{bmatrix} -1 & 1 & & & \\ & -1 & 1 & & \\ & & \ddots & & \\ & & -1 & 1 & \\ & & & -1 & 1 \end{bmatrix}, \tag{6}$$

$$\boldsymbol{\Gamma}_2 = \begin{bmatrix} 1 & -2 & 1 & & & \\ & 1 & -2 & 1 & & \\ & & & \ddots & & \\ & & & 1 & -2 & 1 \\ & & & & 1 & -2 & 1 \end{bmatrix}. \tag{7}$$

Note that L_1 norm regularization is the only norm that favors sparse solutions and results in convex problems. Particularly, L_p norm regularization with $p > 1$ results in a convex problem but does not promote sparsity, whereas that with $p < 1$ promotes sparsity but results in non-convexity.

B. ITERATIVE REWEIGHTED LEAST SQUARES ALGORITHM

Although many algorithms, such as fast iterative shrinkage-threshold algorithm (FISTA) and alternating direction method of multipliers (ADMM), are available to solve the problems formulated in Eqs. (4) and (5), iteratively reweighted least squares algorithm is used in this work [38]–[40]. A least squares problem must be solved for a linear model in each iteration of this method. Numerically efficient algorithms are developed in the next subsection to solve these least squares problems.

First, replace L_1 norm in Eqs. (2) and (3) with a continuously differentiable one.

$$J_1(\{m_k\}) \approx \sum_{k=1}^{n} w_k(\phi_k - m_k)^2 + \lambda \sum_{k=2}^{n} \frac{(m_k - m_{k-1})^2}{\sqrt{(\hat{m}_k - \hat{m}_{k-1})^2 + \delta}}, \tag{8}$$

$$J_2(\{m_k\}) \approx \sum_{k=1}^{n} w_k(\phi_k - m_k)^2 + \mu \sum_{k=3}^{n} \frac{(m_k - 2m_{k-1} + m_{k-2})^2}{\sqrt{(\hat{m}_k - 2\hat{m}_{k-1} + \hat{m}_{k-2})^2 + \delta}}, \tag{9}$$

where the value with an overbar denotes the estimate obtained in the immediate previous iteration, and δ is a positive small number to avoid possible problems of dividing by zero. Accordingly, Eqs. (4) and (5) are approximated by

$$J_1(\boldsymbol{m}) \approx (\boldsymbol{\phi} - \boldsymbol{m})^{\mathrm{T}} \boldsymbol{W} (\boldsymbol{\phi} - \boldsymbol{m}) + \lambda \boldsymbol{m}^{\mathrm{T}} \boldsymbol{\Gamma}_1^{\mathrm{T}} \boldsymbol{D}_1 \boldsymbol{\Gamma}_1 \boldsymbol{m}, \tag{10}$$

$$J_2(\boldsymbol{m}) \approx (\boldsymbol{\phi} - \boldsymbol{m})^{\mathrm{T}} \boldsymbol{W} (\boldsymbol{\phi} - \boldsymbol{m}) + \mu \boldsymbol{m}^{\mathrm{T}} \boldsymbol{\Gamma}_2^{\mathrm{T}} \boldsymbol{D}_2 \boldsymbol{\Gamma}_2 \boldsymbol{m}, \tag{11}$$

$$D_1 = \begin{bmatrix} d_1^1 & & & & \\ & \ddots & & & \\ & & d_i^1 & & \\ & & & \ddots & \\ & & & & d_{k-1}^1 \end{bmatrix}$$

$$d_i^1 = \frac{1}{\sqrt{(\hat{m}_i - \hat{m}_{i-1})^2 + \delta}},$$

$$\boldsymbol{D}_2 = \begin{bmatrix} d_1^2 & & & & \\ & \ddots & & & \\ & & d_i^2 & & \\ & & & \ddots & \\ & & & & d_{k-1}^2 \end{bmatrix}$$

$$d_i^2 = \frac{1}{\sqrt{(\hat{\boldsymbol{m}}_i - 2\hat{\boldsymbol{m}}_{i-1} + \hat{\boldsymbol{m}}_{i-2})^2 + \delta}}.$$

Hence, minimizers of Eqs. (10) and (11) satisfy the following necessary conditions:

$$\left(\boldsymbol{W} + \lambda \boldsymbol{\Gamma}_1^{\mathrm{T}} \boldsymbol{D}_1 \boldsymbol{\Gamma}_1\right) \hat{\boldsymbol{m}}(\lambda) = \boldsymbol{W}\boldsymbol{\phi}, \tag{12}$$

$$\left(\boldsymbol{W} + \mu \boldsymbol{\Gamma}_2^{\mathrm{T}} \boldsymbol{D}_2 \boldsymbol{\Gamma}_2\right) \hat{\boldsymbol{m}}(\mu) = \boldsymbol{W}\boldsymbol{\phi}. \tag{13}$$

Instead of directly solving the numerically efficient algorithms mentioned above (see next subsections for the brief discussion), the special structure of the coefficient matrices is simply adopted. Let superscript (i) denote the ith iteration, whereby the iteration is terminated when $\left|\hat{\boldsymbol{m}}^{(i)} - \hat{\boldsymbol{m}}^{(i-1)}\right|$ is not more than the predetermined small positive constant, such as 0.0001. An initial guess for the iteration can be obtained by letting $\boldsymbol{D}_1/\boldsymbol{D}_2$ be identity matrices.

C. NUMERICALLY EFFICIENT EQUATION SOLVERS

The tridiagonal coefficient matrix $\left(\boldsymbol{W} + \lambda \boldsymbol{\Gamma}_1^{\mathrm{T}} \boldsymbol{D}_1 \boldsymbol{\Gamma}_1\right)$ in Eq. (12) can be expressed as (14), shown at the top of the next page, where d_k denotes the kth diagonal elements of $\boldsymbol{D}_1$. Hence, Thomas algorithm, also called tridiagonal matrix algorithm, is the Gaussian elimination algorithm constructed for the tridiagonal matrix and can be used to solve Eq. (12). First, a forward recursion is performed:

$$c_k = \frac{-\lambda d_k}{w_k + \lambda d_{k-1} + \lambda d_k + \lambda d_{k-1} c_{k-1}} \tag{15}$$

$$k = 2, 3, \cdots, n-1, \quad \text{with } c_1 = \frac{-\lambda d_1}{w_1 + \lambda d_1},$$

$$g_k = \frac{w_k \phi_k + \lambda d_{k-1} g_{k-1}}{w_k + \lambda d_{k-1} + \lambda d_k + \lambda d_{k-1} c_{k-1}}$$

$$k = 2, 3, \cdots, n, \quad \text{with } g_1 = \frac{w_1 \phi_1}{w_1 + \lambda d_1}. \tag{16}$$

$$\begin{bmatrix} w_1+\lambda d_1 & -\lambda d_1 & & & \\ -\lambda d_1 & w_2+\lambda d_1+\lambda d_2 & -\lambda d_2 & & \\ & & \ddots & & \\ & & -\lambda d_{n-2} & w_{n-1}+\lambda d_{n-2}+\lambda d_{n-1} & -\lambda d_{n-1} \\ & & & -\lambda d_{n-1} & w_n+\lambda d_{n-1} \end{bmatrix}, \tag{14}$$

Then, the solution is obtained by performing the following back substitution:

$$\begin{aligned} m_k &= g_k - c_k m_{k+1} \\ k &= n-1, \quad n-2, \cdots, 1, \text{ with } m_n = g_n. \end{aligned} \tag{17}$$

This completes the algorithm development for solving the first-order derivative regularization problem.

Let $\mathbf{\Gamma}_2^{\mathrm{T}} = \left[\, \boldsymbol{\xi}_1 \ \boldsymbol{\xi}_2 \ \cdots \ \boldsymbol{\xi}_{n-2} \,\right], \boldsymbol{\xi}_i = \left[\, \cdots \ \underset{i}{1} \ \underset{i+1}{-2} \ \underset{i+2}{1} \ \cdots \,\right]^T$, we then have the following Cholesky rank-one update formula:

$$\boldsymbol{M} = \left(\boldsymbol{W} + \mu \mathbf{\Gamma}_2^{\mathrm{T}} \boldsymbol{D}_2 \mathbf{\Gamma}_2\right)^{-1} = \left(\boldsymbol{W} + \mu \sum_{k=1}^{n-2} d_k \boldsymbol{\xi}_k \boldsymbol{\xi}_k^{\mathrm{T}}\right)^{-1}, \tag{18}$$

where d_k denotes the kth diagonal elements of $\boldsymbol{D}_2$. Not to be confused with that in the above algorithm, let $\boldsymbol{f} = \left[\,1 \ -2 \ 1\,\right]^T, \boldsymbol{M}_k = \left(\boldsymbol{W} + \mu \sum_{j=1}^{k} d_j \boldsymbol{\xi}_j \boldsymbol{\xi}_j^{\mathrm{T}}\right)^{-1}$ and the 3×3 submatrix of $\boldsymbol{M}_{k-1}$ starting from kth row and kth column be denoted as $\boldsymbol{U}_k$. Then, based on the Shermann–Morrison formula, we have

$$\begin{aligned} \boldsymbol{M}_k &= \boldsymbol{M}_{k-1} - \frac{\mu d_k}{1+\mu d_k \boldsymbol{f}^{\mathrm{T}} \boldsymbol{U}_k \boldsymbol{f}} \begin{bmatrix} 0 & 0 & 0 \\ 0 & \boldsymbol{U}_k \boldsymbol{ff}^{\mathrm{T}} \boldsymbol{U}_k & 0 \\ 0 & 0 & 0 \end{bmatrix} \\ k &= 1, 2, \cdots, n-2, \quad \text{with } \boldsymbol{M}_0 = \boldsymbol{W}^{-1}. \end{aligned} \tag{19}$$

The location of the submatrix $\boldsymbol{U}_k \boldsymbol{ff}^{\boldsymbol{T}} \boldsymbol{U}_k$ in the bracket is the same as that of $\boldsymbol{U}_k$ in $\boldsymbol{M}_{k-1}$, which means that in each iteration, such as that in Eq. (19), only nine elements (a 3×3 submatrix) must be updated. After the final iteration, we have $\boldsymbol{M} = \boldsymbol{M}_{n-2}$. Finally, we have

$$\hat{\boldsymbol{m}}(\mu) = \boldsymbol{MW\phi}. \tag{20}$$

This completes the algorithm development for solving the second-order derivative regularization problem.

D. DETERMINING THE REGULARIZATION COEFFICIENTS BY USING THE BOOTSTRAP TECHNIQUE

Modeling errors are inevitable in empirical models. The modeling errors are assessed by using the bootstrap method [36]. First, select the regularization coefficient corresponding to the minimum modeling error. Then, determine the candidate set of the regularization coefficients. For example,

$$\lambda \text{ or } \mu \in C = \{0.1, 1, 10, 100, \ldots\}.$$

For each coefficient in the candidate set, perform the modeling process described in II. **B** or II.**C**. Define the following normalized residuals (residual of the carrier phase measurement residual)

$$\varpi_k = w_k\left(\phi_k - \hat{m}_k\right), \quad k = 1, 2, \cdots, n. \tag{21}$$

This residual series is homoscedastic. We randomly sample from the above normalized residual series with a replacement to obtain series $\{\varphi_k\}$. Add series $\{\varphi_k / w_k\}$ to $\left\{\hat{m}_k\right\}$ to obtain a resampled measurement vector $\tilde{\boldsymbol{\phi}}$. Repeat this resampling process B times. For example, $B = 50$. For the bth resampled measurement vector, $1 \leq b \leq B$. Perform the modeling described in II. **B** or II.**C**. Let the corresponding estimate be denoted as $\hat{\boldsymbol{m}}_b(\lambda)$ or $\hat{\boldsymbol{m}}_b(\mu)$. The argument λ/μ is introduced intentionally to denote the dependence on the regularization coefficients. Let the following average be the final estimate for the corresponding regularization coefficients

$$\begin{aligned} \hat{\boldsymbol{m}}(\lambda) &= \frac{1}{B+1} \sum_{b=0}^{B} \hat{\boldsymbol{m}}_b(\lambda) \\ \hat{\boldsymbol{m}}(\mu) &= \frac{1}{B+1} \sum_{b=0}^{B} \hat{\boldsymbol{m}}_b(\mu). \end{aligned} \tag{22}$$

The subscript $b = 0$ denotes the solution obtained in II.**A** or II. **B** by using the original measurement. The solution in Eq. (22), often called bootstrap estimate, is generally better than the one obtained by using only the original measurement. Define the following error statistics with the following:

$$\begin{aligned} err(\lambda) &= \frac{1}{nB} \sum_{b=0}^{B} \left[\hat{\boldsymbol{m}}_b(\lambda) - \hat{\boldsymbol{m}}(\lambda)\right]^{\mathrm{T}} \left[\hat{\boldsymbol{m}}_b(\lambda) - \hat{\boldsymbol{m}}(\lambda)\right] \\ err(\mu) &= \frac{1}{nB} \sum_{b=0}^{B} \left[\hat{\boldsymbol{m}}_b(\mu) - \hat{\boldsymbol{m}}(\mu)\right]^{\mathrm{T}} \left[\hat{\boldsymbol{m}}_b(\mu) - \hat{\boldsymbol{m}}(\mu)\right]. \end{aligned} \tag{23}$$

These error statistics denote the overall modeling errors with different modeling strategies (first- or second-order derivative regularization) and hyper parameters λ/μ. Finally, the regularization coefficient is determined as follows:

$$\begin{aligned} \hat{\lambda} &= \arg\min_{\lambda \in C} err(\lambda) \\ \hat{\mu} &= \arg\min_{\mu \in C} err(\mu). \end{aligned} \tag{24}$$

The estimate based on the coefficient in Eq. (22) is the final estimate, which is used to correct the measurement at the same time of the future period.

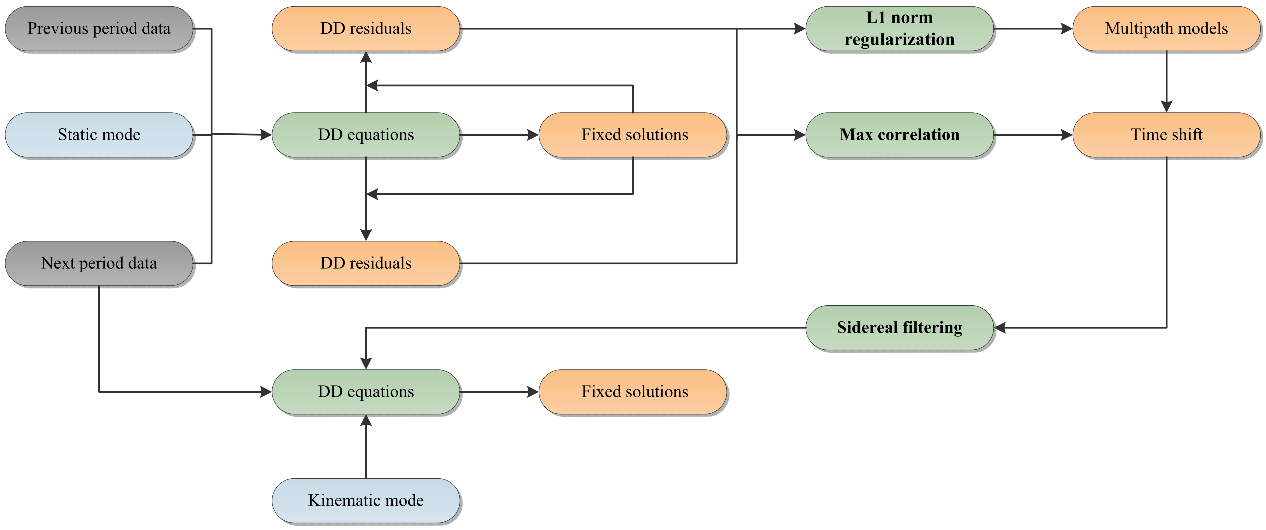

FIGURE 1. Flowchart of the proposed multipath error modeling method.

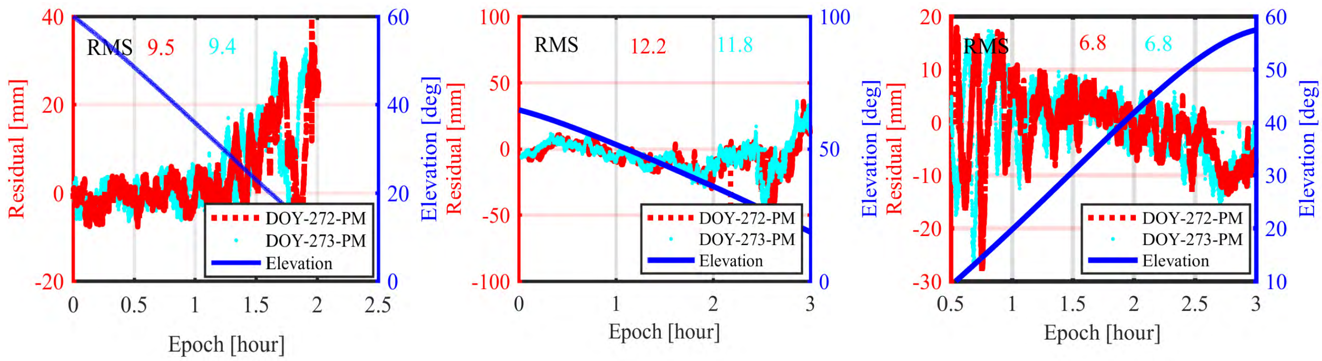

FIGURE 2. Carrier phase residuals of G02 (left), G05 (middle), G21(right) under static mode on DOY-272-273-PM. (The RMS value with a different color belongs to the curve of the same color.)

III. DATA PROCESSING RESULTS

Two datasets were conducted on the rooftop of the School of Environment Science and Spatial Informatics in China University of Mining and Technology to evaluate the effectiveness of the proposed method in multipath mitigation. One dataset was collected from 14:00 to 18:00 on 29 September 2017 and 30 September 2017 and named DOY-272-PM and DOY-273-PM, respectively with a sampling rate of 1 Hz and 10° elevation mask angle. Another dataset was collected from 8:00 to 11:00 on 7 October 2017 and 8 October 2017 and named DOY-280-AM and DOY-281-AM, respectively, under the same observation settings. One antenna was mounted at an empty corner with an unobstructed environment, which was used as the base station. Another antenna was placed approximately 5 m away from the southeast direction of a white wall, which was used as the rover station. The two GNSS receivers were Trimble R10 units and the length of the baseline is around 62.210 m. To ensure that the base station was not affected by multipath effects and that the rover station had a significant multipath effect, we turned off the anti-multipath function of the rover station as the function of the base station was switched on. The processing software of mitigating multipath error was developed based on GNSS data processing software RTKLIB [41]. Multipath mitigation based on double-differenced (DD) sidereal filtering requires the following steps [42]. First, process the previous period dataset under static mode, and the final baseline vector can be estimated after ambiguities are resolved. Second, substitute the integer ambiguities and baseline vector back to the DD equation epoch by epoch. We can obtain DD residuals in the DD multipath and noise for each satellite. Third, we can establish DD multipath models after DD residuals are denoised by using the method proposed in Section **II**. Finally, apply the extracted multipath model to the next period data with time shift. The baseline vector at each epoch is estimated independently in the kinematic mode with ambiguities fixed. **Fig. 1** shows the flowchart of the proposed multipath mitigation approach based on L_1 norm regularization.

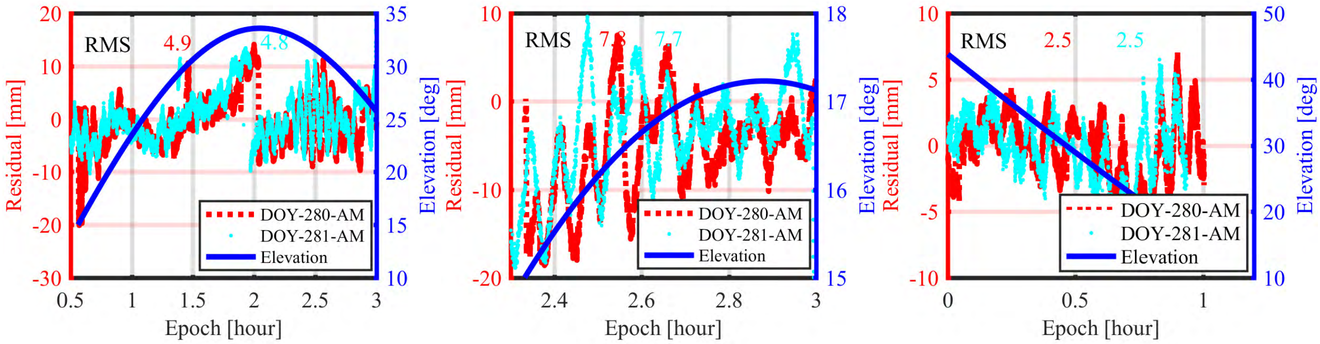

FIGURE 3. Carrier phase residuals of G12 (left), G25 (middle), G28(right) under kinematic mode DOY-280-281-AM. (The RMS value with a different color belongs to the curve of the same color.)

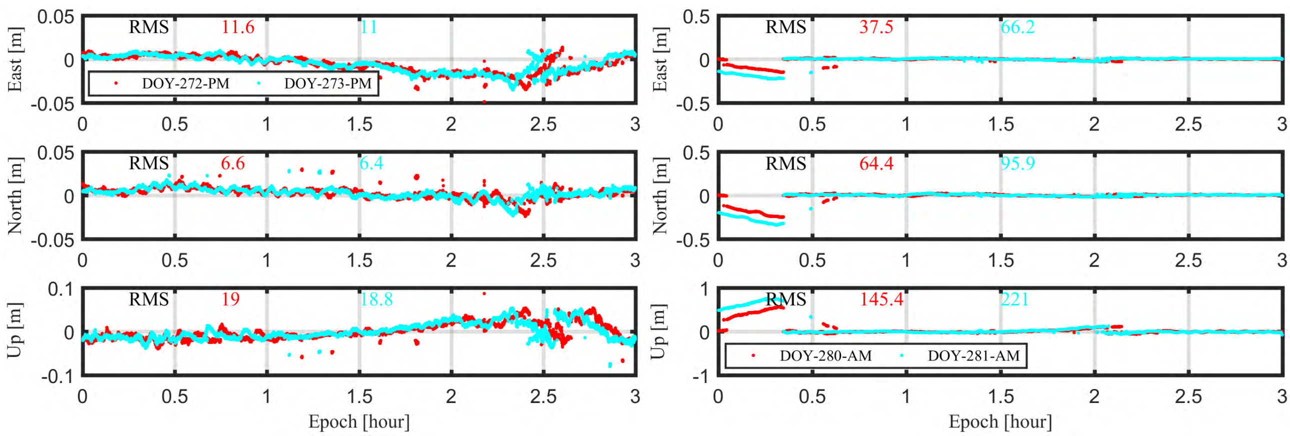

FIGURE 4. Original coordinate residual series in EAST, NORTH, and UP on DOY-272-273-PM (left) and DOY-280-281-AM (right) under kinematic mode. (The RMS value with a different color belongs to the curve of the same color.)

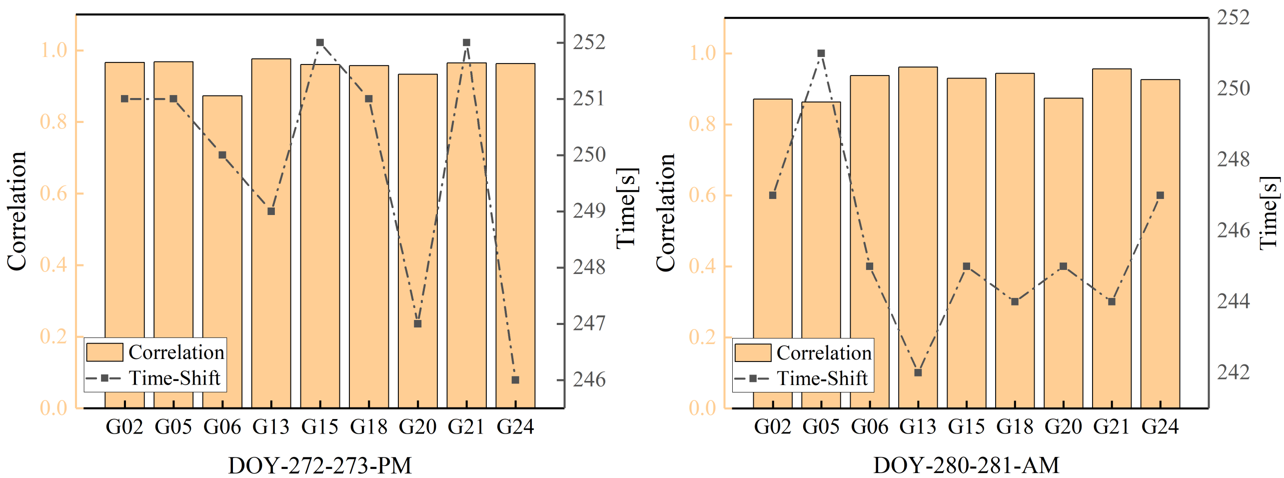

FIGURE 5. Correlation of residuals (bar) and residual time–shift (plot) corresponding to the maximum correlation coefficients of different GPS satellites on DOY-272-PM (left) and DOY-280-AM (right), respectively.

The three commonly used methods for estimating the multipath repeat time [20] are orbit repeat time method [18], ARTA [17], [19], and residual correlation method [43]. More details can be found in reference [20] on the comparison of derived multipath repeat time estimates by using the three methods. Sidereal filtering has been well developed and widely applied and most of the existing methods are based on transforming double-difference to single-difference residuals

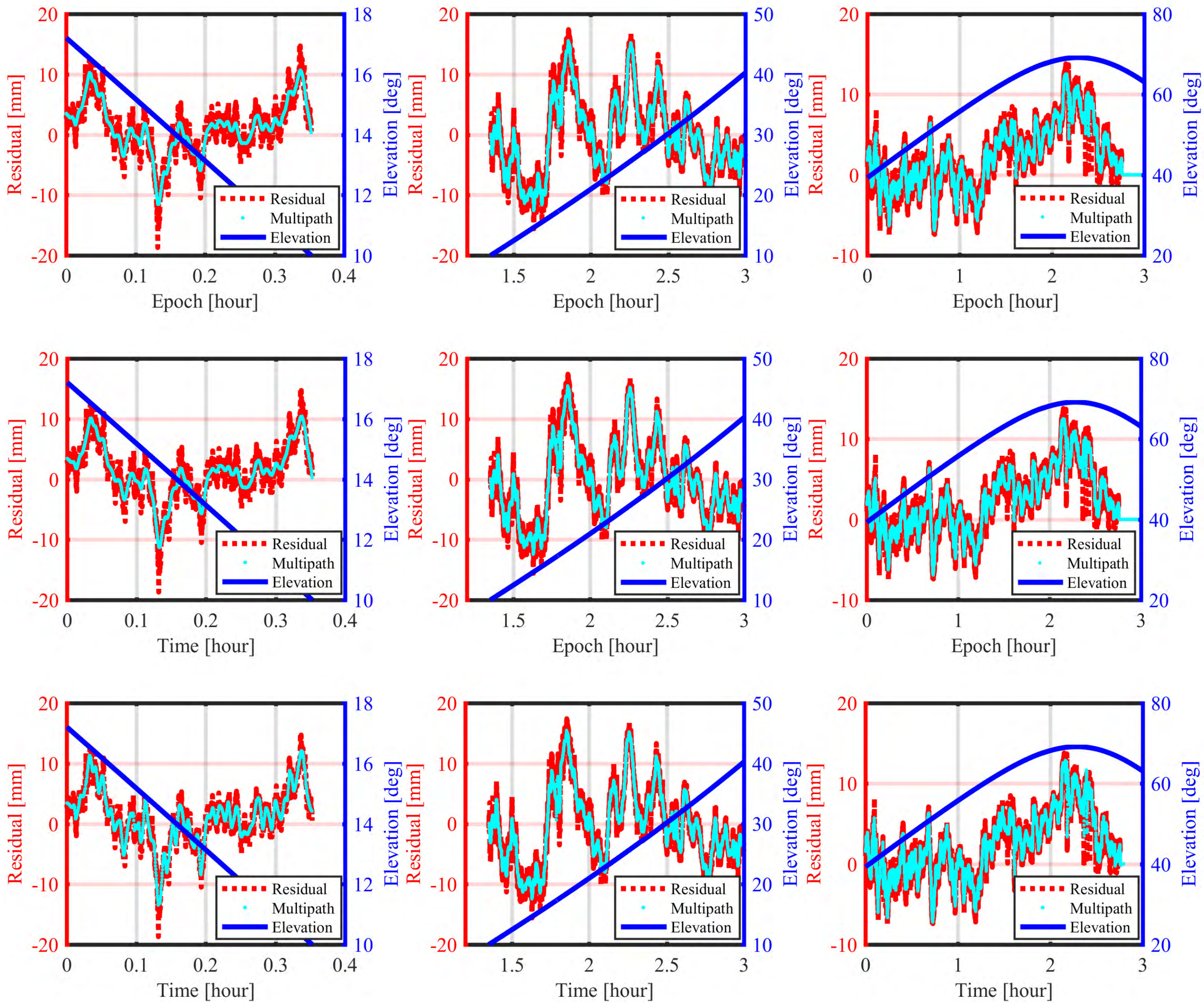

FIGURE 6. Carrier phase residuals and multipath error extracted by using first- (top) and second-order (middle) regularization methods and wavelet filter (bottom) of G06 (left), G18 (middle), G20 (right) on DOY-272-PM.

following the approach proposed by Alber *et al.* [44], such as those found in [16], [42], and [45]. The single-difference operation has the advantage of processing data from each satellite separately, rather than working with a pair of satellites. Directly modeling double-difference multipath error has also been studied [43]. Without loss of generality in this work, we use residual correlation method to calculate the multipath repeat time following the double-difference operation mode.

On the basis of the steps shown in **Fig. 1**, we calculated the L_1 phase residuals of different GPS satellites (also applicable to L_2 measurements). For short baseline experiments, posterior DD residuals mainly consist of DD multipath errors and measurement noises. Thus, fluctuations of DD residuals will demonstrate the DD multipath characteristics. In the observation domain, the carrier phase residuals of G02, G05, G21 and G12, G25, G28 under static and kinematic modes on DOY-272-PM, DOY-273-PM, and DOY-280-AM, DOY-281-AM, are shown in **Fig. 2–3**, respectively. **Fig. 4** shows the original baseline vector residuals, which are the DD multipath error in the position domain, in EAST, NORTH, and UP on DOY-272-PM, DOY-273-PM, and DOY-280-AM, DOY-281-AM under kinematic mode, respectively. Root mean square (RMS) of residuals is also displayed in the top corner. The first day operates under static mode, thereby ensuring that ambiguities are fixed in most epochs and residuals only contain multipath error and noise. Kinematic mode is followed in the second day as each epoch is treated separately. Common parameters cannot affect the level of multipath error [43]. The figures show that regardless of the observation or position domain, the residuals (multipath error) almost repeat themselves in every sidereal day on consecutive days. The periodical repeatability phenomenon of the multipath signal is due to the periodical motion of a satellite. Hence, the assumption is that the station environment remains unchanged for

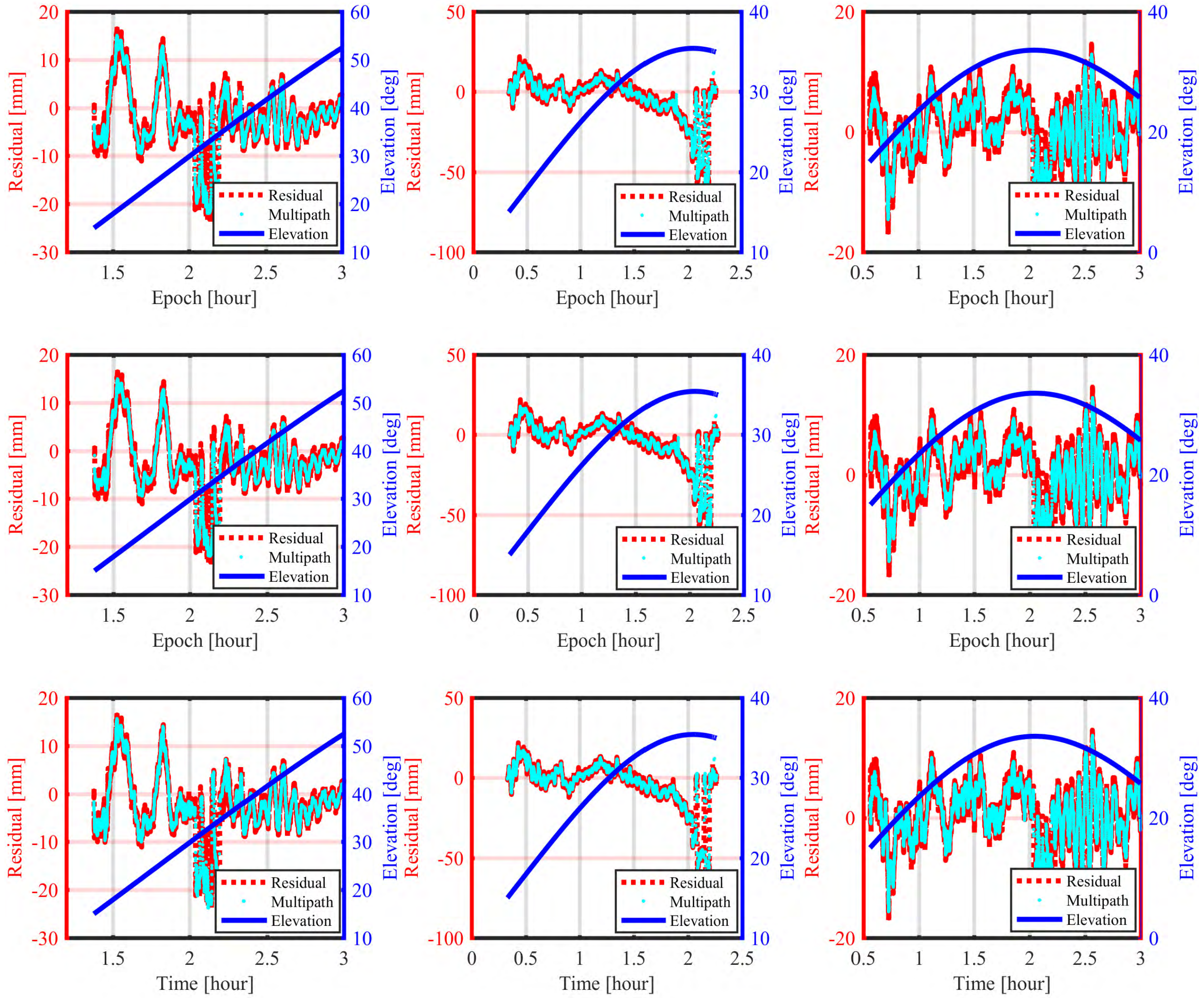

FIGURE 7. Carrier phase residuals and multipath error extracted by using first- (top) and second-order (middle) regularization methods and wavelet filter (bottom) of G05 (left), G09 (middle), G12 (right) on DOY-280-AM.

subsequent days. **Fig. 4** presents that the baseline vector residuals in the first half hour on DOY-280-AM and DOY-281-AM was abnormal, which may be caused by the signal loss of lock, and the ambiguities are not fixed.

As mentioned earlier, sidereal filter is used to mitigate the multipath error, and residual correlation method is used to calculate the multipath repeat time. Normally, shift time represents the multipath repeat time when the consecutive day residual series has a maximal correlation coefficient. **Fig. 5** shows the time shifts of the measurement residual corresponding to the maximum correlation coefficients and statistics. The mean residual time shifts where correlation coefficients reach maximum value is 248 s, and the mean of correlation coefficients are as high as 0.921 in spite of the existence of uncorrelated noises on consecutive days. Thus, we can mitigate multipath effects by using previously developed multipath models based on orbital repeat time due to the remarkable correlation from the sidereal filtering method.

The multipath signals are extracted by using the proposed sparsity-promoting regularization method in this study. Other methods [9], [46], [47] with the same aims have been proposed in the literature. Among them, wavelet threshold denoising method is chosen as an example in data analysis to obtain an intuitive appreciation for the relative performance of the developed method. G06, G18, and G20 on Doy-272-PM and G05, G09 and G12 on Doy-280-AM are taken as examples. **Fig. 6–7** show the extracted multipath signals with first- and second-order regularization, respectively. From these figures, the following conclusions can be drawn. First, the multipath signals can be extracted correctly by first- and second-order regularization constraint, wherein the multipath

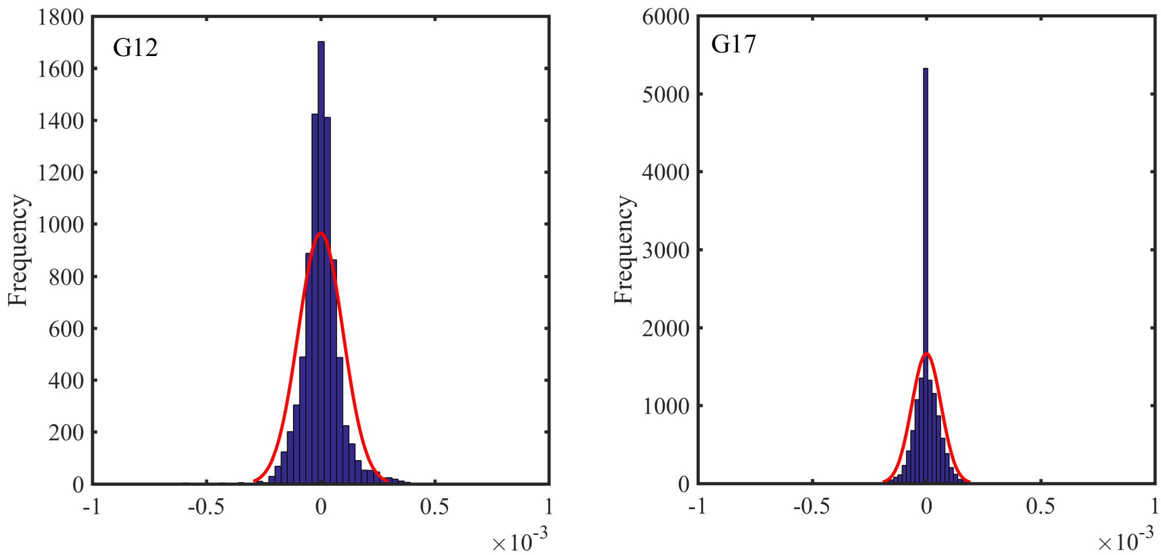

FIGURE 8. Frequency of zero for $m_k - m_{k-1}$.

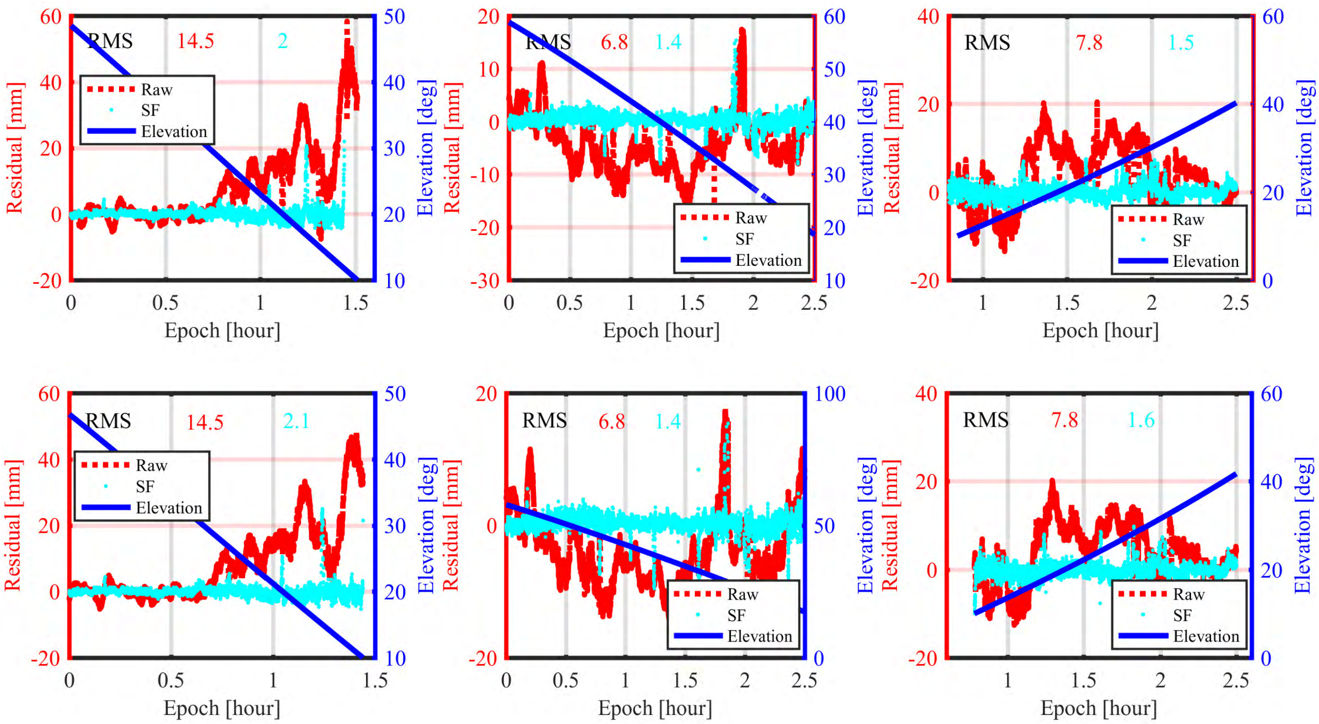

FIGURE 9. Carrier phase residuals of G02, G05, and G18 before and after applying sidereal filtering on DOY-273-PM: raw vs. mitigated with first-order regularization (top); raw vs. mitigated with wavelet filtering (bottom). (The RMS value with a different color belongs to the curve of the same color.)

signals are relatively smoother than raw measurement residuals. The second observation implies the denoising effect of the proposed method. The third presents that first-order regularization method is only slightly better than the second-order regularization method, which is consistent with the fact that reduced smooth property of multipath signals. For the sake of brevity, only the results from first-order regularization method are shown as second-order regularization method obtains similar results and leads to the same conclusion. Compared with classical wavelet filtering, the extracted multipath error curves by using the proposed methods can approximately coincide with the use of wavelet filtering. **Fig. 6–7**

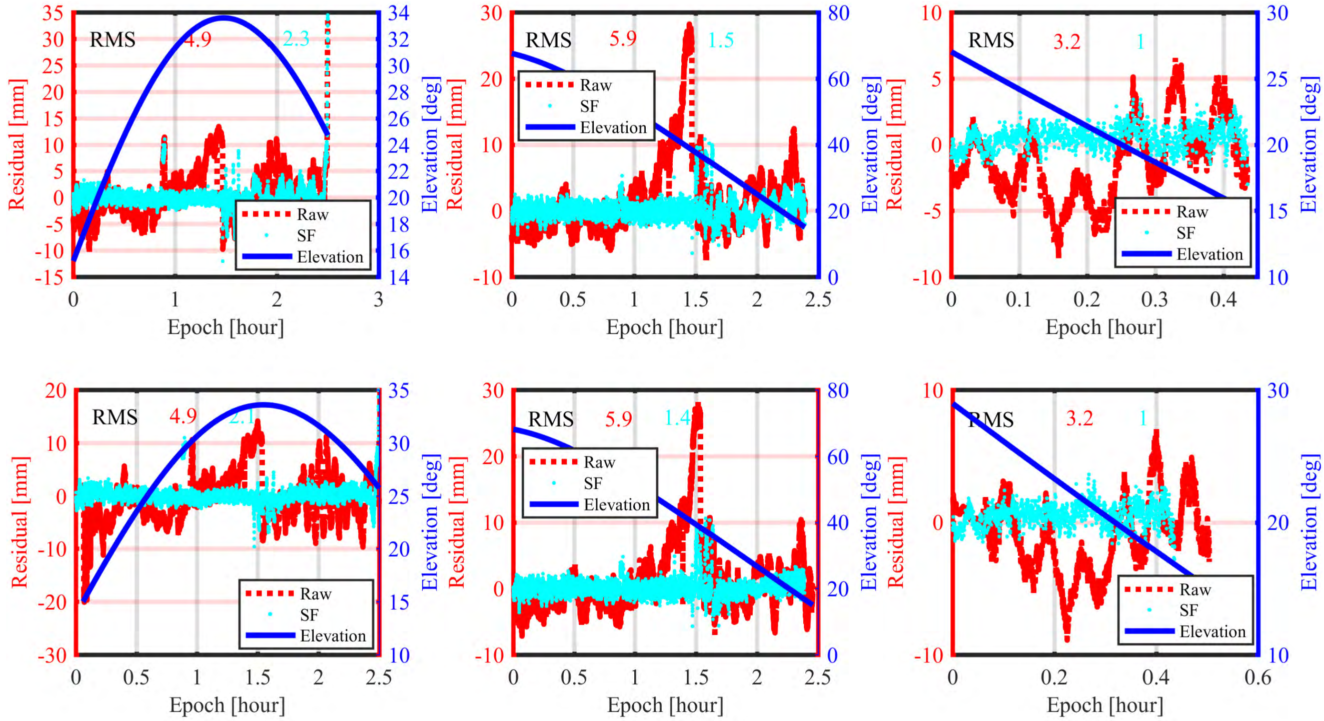

FIGURE 10. Carrier phase residuals of G12, G18, and G28 before and after applying sidereal filtering on DOY-273-PM: raw vs. mitigated with first-order regularization (top); raw vs. mitigated with wavelet filtering (bottom). (The RMS value with a different color belongs to the curve of the same color.)

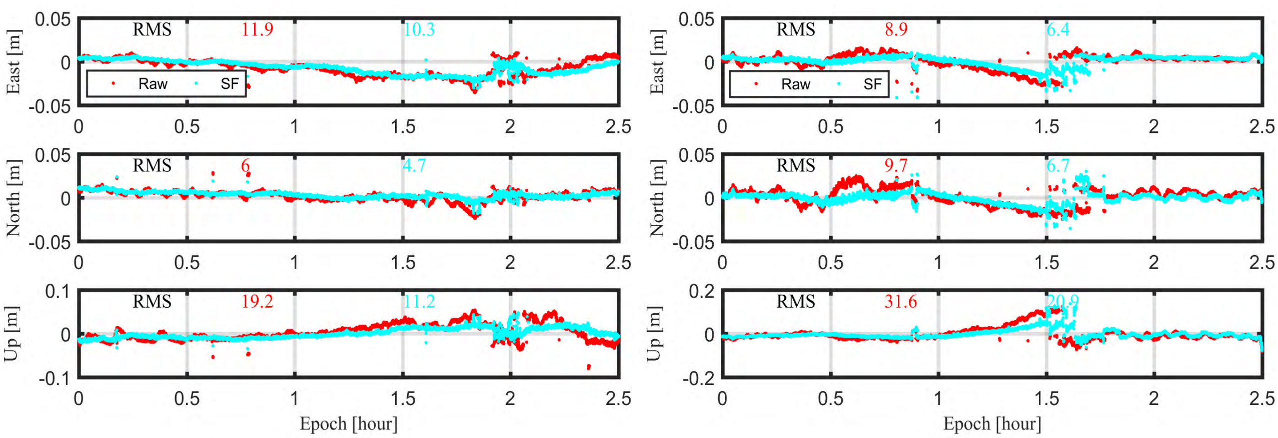

FIGURE 11. Baseline coordinate residuals in East, North, and Up directions by using raw measurements (red) and measurements corrected by using sidereal filtering with first-order regularization (cyan) on DOY-273-PM and DOY-281-AM, respectively. (The RMS value with a different color belongs to the curve of the same color.)

show the effectiveness of regularization method. In **Fig. 8**, it is clearly shown that there is a significant part of between-epoch different in the models constructed.

After the multipath signals are extracted correctly, the two key steps of sidereal filter are completed, namely, multipath model and repeat time. Thus, the multipath model is subtracted from the obtained time shift by using the last period data to the current period data. **Fig. 9–10** show the posterior DD residuals before and after application of sidereal filter of G02, G05, and G18 on DOY-273-PM and G12, G17, and G28 on DOY-281-AM, respectively. The figures show that multipath error can be mitigated effectively and that posterior residuals only reflect the random characteristics after sidereal filter (cyan lines). Hence, effectiveness of the proposed method is further verified. The direct consequence of this efficacy is the smoother coordinate series obtained with multipath mitigation by using wavelet filtering first-order regularization than those without mitigation (**Fig. 11–12**),

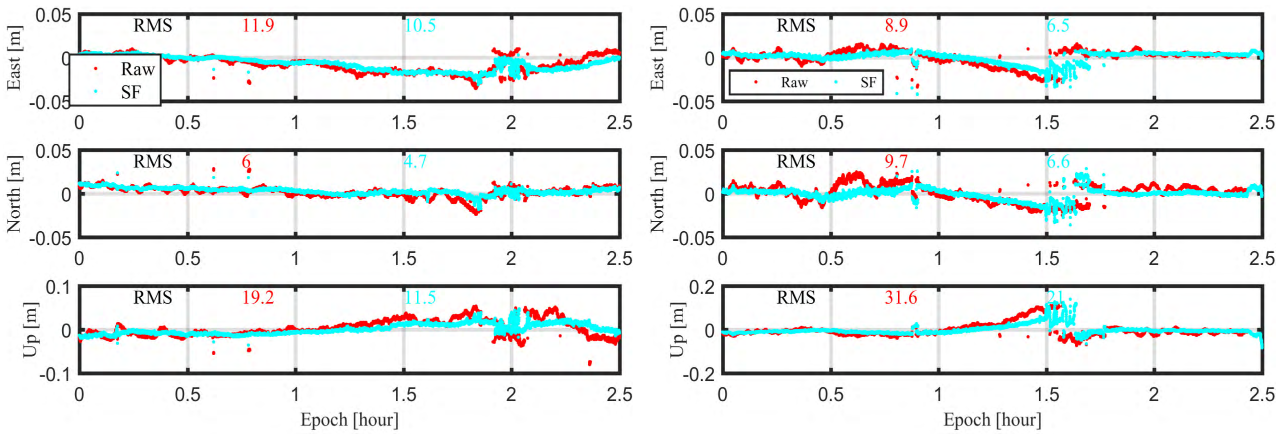

FIGURE 12. Baseline coordinate residuals in East, North, and Up directions by using raw measurements (red) and measurements corrected by using sidereal filtering with wavelet filtering (cyan) on DOY-273-PM and DOY-281-AM, respectively. (The RMS value with a different color belongs to the curve of the same color.)

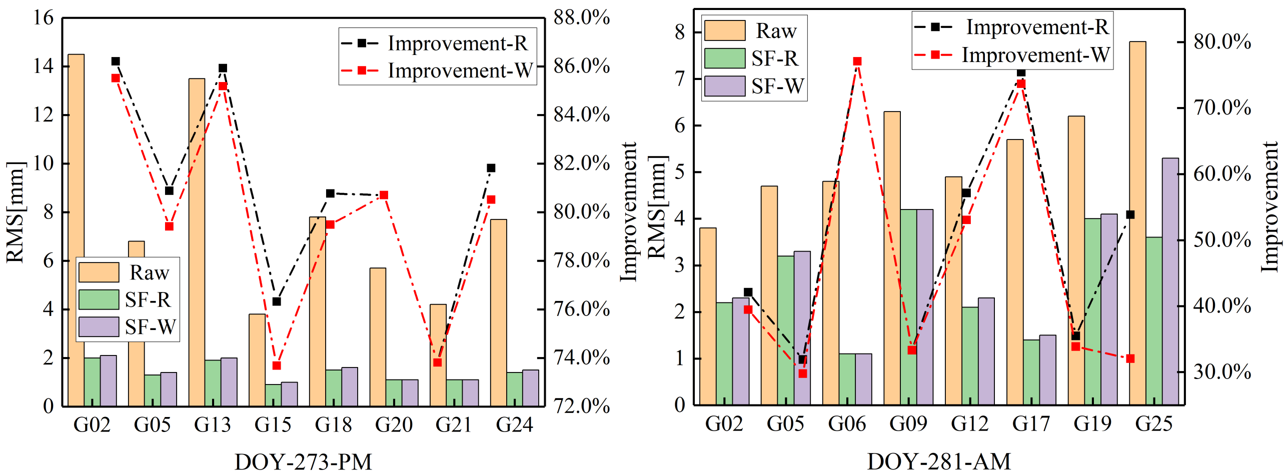

FIGURE 13. RMS (bar) and improvement (plot) of measurement residuals before and after multipath mitigation by using sidereal filtering with first-order regularization (SF–R) and wavelet filtering (SF–W) on DOY-273-PM and DOY-281-AM, respectively.

TABLE 1. RMS (mm) and improvement of baseline coordinate residuals before and after sidereal filtering with first-order regularization and wavelet filtering.

	DOY-273-PM					DOY-281-AM				
	Raw	R.	W.	Impro.R	Impro.W	Raw	R.	W.	Impro.R	Impro.W
East	11.9	10.3	10.5	13.4%	11.8%	8.9	6.4	6.5	28.1%	26.9%
North	6.0	4.7	4.7	21.7%	21.7%	9.7	6.7	6.6	30.9%	32.0%
Up	19.2	11.2	11.5	41.7%	40.1%	31.6	20.9	21.0	33.9%	33.5%
Mean	-	-	-	25.6%	24.5%	-	-	-	31.0%	30.8%

and RMS of the residuals are displayed in the top corner. **Fig. 13** and **TABLE 1–2** show the statistics of residuals in the observation and position domains. The figure and tables show that (1) the ambiguity fixed rate before and after sidereal filter and multipath mitigation increased the fixed rate from 94.8% to 98.2% on DOY-273-PM and 93.7% to 97.7% on DOY-281-AM, respectively; (2) the cyan lines are relatively smoother and less outlying than the original results, especially during 15:30 to 16:00 on DOY-273-PM. Smoothness of the calculated coordinates by using the corrected measurements is improved significantly compared with those from raw measurements; (3) the average improvements along East, North, and Up directions after multipath mitigation by using wavelet filter and first-order regularization are 19.4%, 26.8%,

TABLE 2. Fixed rate values of ambiguity before and after multipath mitigation on DOY-273-PM and DOY-281-AM.

	DOY-273-PM		DOY-281-AM	
	Fixed-rate	Improvement	Fixed-rate	Improvement
Raw	94.8%		93.7%	
Wavelet filter	98.1%	3.3%	97.6%	3.9%
Proposed method	98.2%	3.4%	97.7%	4.0%

36.8% and 20.8%, 26.3%, 37.8%, respectively. These results show the efficacy of the proposed method. The experimental results validate the effectiveness of the proposed method.

IV. CONCLUSION

Multipath mitigation is an important step in GNSS data processing for high precision geodetic/geophysical and engineering applications. This work investigates the characteristics of multipath effect and provides an alternative strategy to extract an accurate multipath model. A new sidereal filtering with sparsity promoting regularization is proposed to mitigate multipath error for static short baseline GNSS applications. Two regularization terms, namely the first order and the second order differences, are considered and compared. These regularization terms are introduced to constrain the complexity of the resulted model and hence to promote a simpler model with relatively better generalization capability. The regularization parameters, namely the Lagrange multipliers, are optimized objectively using bootstrap method. Two short baselines with different sampling rates and different processing modes have been used to assess the characteristics of multipath effect and the performance of the proposed method. From the experiment result, the merit of the proposed method is demonstrated. The main conclusions are summarized from experiment results as follows:

1. No matter in observation domain or in position domain, the residuals (multipath error) almost repeated themselves every sidereal day on consecutive days. The periodical repeatability phenomenon of multipath signal results from the periodical motion of a satellite.

2. The multipath signals can be modeled well by the sparsity promoting regularization methods and the second-order regularization method is only slightly better than the first-order.

3. After sidereal filtering, in observation, the proposed method can improve the RMS of carrier phase measurement residuals by about 66.7% compared with the result without multipath mitigation in two datasets. In position domain, the positioning precision is improved by about 20.8%, 26.3%, 37.8% in East/North/Up directions, respectively.

4. After multipath mitigation, the ambiguity fixed rate is improved 3.7% in average in kinematic mode.

As a final note, though double difference mode is followed in this work, the proposed method can be easily applied to single and zero difference modes, provided system error terms rather than multipath errors can be appropriately taken care of.

ACKNOWLEDGMENT

The authors are grateful to three reviewers for providing many valuable suggestions.

REFERENCES

[1] T.-H. Yi, H.-N. Li, and M. Gu, "Characterization and extraction of global positioning system multipath signals using an improved particle-filtering algorithm," *Meas. Sci. Technol.*, vol. 22, no. 7, May 2011, Art. no. 075101.

[2] W. Li and Y. Shen, "The consideration of formal errors in spatiotemporal filtering using principal component analysis for regional GNSS position time series," *Remote Sens.*, vol. 10, no. 4, p. 534, Mar. 2018.

[3] C. Liu, P. Lin, X. Zhao, and J. Gao, "Reducing GPS carrier phase errors in the measurement and position domains for short-distance static relative positioning," *Acta Geodaetica et Geophys.*, vol. 51, no. 1, pp. 81–93, Mar. 2015.

[4] M. Cai *et al.*, "Reduction of kinematic short baseline multipath effects based on multipath hemispherical map," *Sensors*, vol. 16, no. 10, p. 1677, Oct. 2016.

[5] G. Chang, T. Xu, and Q. Wang, "Baseline configuration for GNSS attitude determination with an analytical least-squares solution," *Meas. Sci. Technol.*, vol. 27, no. 12, Nov. 2016, Art. no. 125105.

[6] K. Yu, W. Ban, X. Zhang, and X. Yu, "Snow depth estimation based on multipath phase combination of GPS triple-frequency signals," *IEEE Geosci. Remote Sens. Lett.*, vol. 53, no. 9, pp. 5100–5109, Sep. 2015.

[7] H. Liu, D. Li, Y. Zhou, and T. Truong, "Simultaneous radio frequency and wideband interference suppression in SAR signals via sparsity exploitation in time–frequency domain," *IEEE Trans. Geosci. Remote Sens.*, vol. 56, no. 10, pp. 5780–5793, Oct. 2018.

[8] S. Barbarossa and V. Petrone, "Analysis of polynomial-phase signals by the integrated generalized ambiguity function," *IEEE Trans. Signal Process.*, vol. 45, no. 2, pp. 316–327, Feb. 1997.

[9] M. Su, J. Zheng, Y. Yang, and Q. Wu, "A new multipath mitigation method based on adaptive thresholding wavelet denoising and double reference shift strategy," *GPS Solutions*, vol. 22, p. 40, Apr. 2018.

[10] L. Lau, "Wavelet packets based denoising method for measurement domain repeat-time multipath filtering in GPS static high-precision positioning," *GPS Solutions*, vol. 21, no. 2, pp. 461–474, Apr. 2017.

[11] D. Wang, X. Meng, C. Gao, S. Pan, and Q. Chen, "Multipath extraction and mitigation for bridge deformation monitoring using a single-difference model," *Adv. Space Res.*, vol. 60, no. 12, pp. 2882–2895, Dec. 2017.

[12] G. Pugliano, U. Robustelli, F. Rossi, and R. Santamaria, "A new method for specular and diffuse pseudorange multipath error extraction using wavelet analysis," *GPS Solutions*, vol. 20, no. 3, pp. 499–508, Jul. 2016.

[13] D. W. Zheng, P. Zhong, X. L. Ding, and W. Chen, "Filtering GPS time-series using a Vondrak filter and cross-validation," *J. Geodesy*, vol. 79, nos. 6–7, pp. 363–369, Aug. 2005.

[14] W. Dai, D. Huang, and C. Cai, "Multipath mitigation via component analysis methods for GPS dynamic deformation monitoring," *GPS Solutions*, vol. 18, no. 3, pp. 417–428, Jul. 2014.

[15] J. Wang *et al.*, "Reducing GPS carrier phase errors with EMD-wavelet for precise static positioning," *Surv. Rev.*, vol. 41, no. 312, pp. 152–161, Jul. 2009.

[16] Q. Zhang, W. Yang, S. Zhang, and X. Liu, "Characteristics of BeiDou navigation satellite system multipath and its mitigation method based on Kalman filter and rauch-tung-striebel smoother," *Sensors*, vol. 18, no. 1, p. E198, Jan. 2018.

[17] D. C. Agnew and K. M. Larson, "Finding the repeat times of the GPS constellation," *GPS Solutions*, vol. 11, no. 1, pp. 71–76, Jan. 2006.

[18] K. Choi, A. Bilich, K. M. Larson, and P. Axelrad, "Modied sidereal filtering: Implications for high-rate GPS positioning," *Geophys. Res. Lett.*, vol. 31, no. 22, pp. 1–4, Nov. 2004.

[19] K. M. Larson, A. Bilich, and P. Axelrad, "Improving the precision of high-rate GPS," *J. Geophys. Res. Atmos.*, vol. 112, no. B5, pp. 1–11, May 2007.
[20] M. Wang, J. Wang, D. Dong, H. Li, L. Han, and W. Chen, "Comparison of three methods for estimating GPS multipath repeat time," *Remote Sens.*, vol. 10, no. 2, p. 6, Jan. 2018.
[21] D. Dong *et al.*, "Mitigation of multipath effect in GNSS short baseline positioning by the multipath hemispherical map," *J. Geodesy*, vol. 90, no. 3, pp. 255–262, Mar. 2016.
[22] T. Fuhrmann, X. Luo, A. Knöpfler, and M. Mayer, "Generating statistically robust multipath stacking maps using congruent cells," *GPS Solutions*, vol. 19, no. 1, pp. 83–92, Jan. 2015.
[23] A. K. Reichert and P. Axelrad, "Carrier-phase multipath corrections for GPS-based satellite attitude determination," *Navigation*, vol. 48, no. 2, pp. 76–88, Jun. 2001.
[24] J.-Y. Guo, G.-W. Li, Q.-L. Kong, and S.-Y. Wang, "Modeling GPS multipath effect based on spherical cap harmonic analysis," *Trans. Nonferrous Met. Soc. China*, vol. 24, no. 6, pp. 1874–1879, Jun. 2014.
[25] Y. Yang *et al.*, "Preliminary assessment of the navigation and positioning performance of BeiDou regional navigation satellite system," *Sci. China Earth Sci.*, vol. 57, no. 1, pp. 144–152, Jan. 2014.
[26] A. N. Tikhonov and V. Y. Arsenin, *Solutions of Ill-Posed Problems*. New York, NY, USA: Wiley, 1977.
[27] T. Hastie, *Statistical Learning with Sparsity: The Lasso and Generalizations*. London, U.K.: CRC Press, 2015.
[28] R. Tibshirani, "Regression shrinkage and selection via the lasso," *J. Roy. Stat. Soc. B (Methodol.)*, vol. 58, no. 1, pp. 267–288, 1996.
[29] D. L. Donoho, "De-noising by soft-thresholding," *IEEE Trans. Inf. Theory*, vol. 41, no. 3, pp. 613–627, May 1995.
[30] S. Osher, L. Rudin, and E. Fatemi, "Nonlinear total variation based noise removal algorithms," *Phys. D*, vol. 60, no. 1, pp. 259–268, 1992.
[31] M. E. Tipping, "Sparse Bayesian learning and the relevance vector machine," *J. Mach. Learn. Res.*, vol. 1, pp. 211–244, Jun. 2001.
[32] Y. Yu, Z. Sun, W. Zhu, and J. Gu, "A homotopy iterative hard thresholding algorithm with extreme learning machine for scene recognition," *IEEE Access*, vol. 6, pp. 30424–30436, 2018.
[33] C. M. Bishop, *Pattern Recognition and Machine Learning* (Information Science and Statistics). New York, NY, USA: Springer-Verlag, 2006.
[34] E. J. Candès and M. B. Wakin, "An introduction to compressive sampling," *IEEE Signal Process. Mag.*, vol. 25, no. 2, pp. 21–30, Mar. 2008.
[35] L. I. Rudin *et al.*, "Nonlinear total variation based noise removal algorithms," in *Proc. 11th Int. Conf. Center Nonlinear Stud. Exp. Math., Comput. Issues Nonlinear Sci., Comput. Issues Nonlinear Sci.*, 1992.
[36] B. Efron and R. J. Tibshirani, *An Introduction to the Bootstrap*. London, U.K.: CRC press, 1993.
[37] F. Xiaoyu, L. Qiusheng, and S. Baoshun, "Compressed sensing MRI with phase noise disturbance based on adaptive tight frame and total variation," *IEEE Access*, vol. 5, pp. 19311–19321, 2017.
[38] I. Daubechies, R. DeVore, M. Fornasier, and C. S. Güntürk, "Iteratively reweighted least squares minimization for sparse recovery," *Commun. Pure Appl. Math.*, vol. 63, no. 1, pp. 1–38, Jan. 2010.
[39] P. W. Holland and R. E. Welsch, "Robust regression using iteratively reweighted least-squares," *Commun. Statist.-Theory Methods*, vol. 6, no. 9, pp. 813–827, Jun. 1977.
[40] B. Wohlberg and P. Rodriguez, "An iteratively reweighted norm algorithm for minimization of total variation functionals," *IEEE Signal Process. Lett.*, vol. 14, no. 12, pp. 948–951, Dec. 2007.
[41] T. Takasu and A. Yasuda, "Development of the low-cost RTK-GPS receiver with an open source program package RTKLIB," in *Proc. Int. Symp. GPS/GNSS Jeju Korea*, Nov. 2009, pp. 4–6.
[42] S. R. Ye, D. Chen, Y. Liu, P. Jiang, W. Tang, and P. Xia, "Carrier phase multipath mitigation for BeiDou navigation satellite system," *GPS Solutions*, vol. 19, no. 4, pp. 545–557, Oct. 2014.
[43] A. E. Ragheb, P. J. Clarke, and S. J. Edwards, "GPS sidereal filtering: Coordinate- and carrier-phase-level strategies," *J. Geodesy*, vol. 81, no. 5, pp. 325–335, May 2006.
[44] C. Alber, R. Ware, C. Rocken, and J. Braun, "Obtaining single path phase delays from GPS double differences," *Geophys. Res. Lett.*, vol. 27, no. 17, pp. 2661–2664, Sep. 2000.
[45] P. Zhong, X. Ding, L. Yuan, Y. Xu, K. Kwok, and Y. Chen, "Sidereal filtering based on single differences for mitigating GPS multipath effects on short baselines," *J. Geodesy*, vol. 84, no. 2, pp. 145–158, Feb. 2009.
[46] W. Ye, J. Fang, and J. Li "Intelligent identification and mitigation of GNSS multipath errors using adaptive BOCPD," *Aerosp. Sci. Technol.*, vol. 70, pp. 453–460, Nov. 2017.
[47] Q. J. Zhang and K.-P. Schwarz, "Estimating double difference GPS multipath under kinematic conditions," in *Proc. Position, Location Navigat. Symp.-(PLANS)*, Apr. 1996, pp. 285–291.

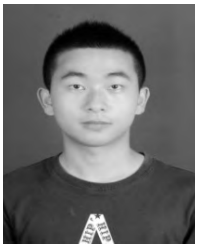

CHAO CHEN received the B.Sc. degree in surveying and mapping engineering from the Anhui University of Science and Technology, Huainan, China, in 2017. He is currently pursuing the Ph.D. degree in geodesy with the School of Environmental Science and Spatial Informatics, China University of Mining and Technology. His research interests include GNSS data processing, inertial navigation, and optimal estimation.

GUOBIN CHANG was born in Heze, China, in 1984. He received the bachelor's degree and the Ph.D. degree in navigation, guidance and control from the Naval University of Engineering, Wuhan, China, in 2006 and 2011, respectively.

From 2012 to 2017, he was a Navigation Engineer with the Tianjin Institute of Hydrographic Surveying and Charting, Tianjin, China. Since 2017, he has been an Associate Professor with the School of Environmental Science and Spatial Informatics and NASG Key Laboratory of Land Environment and Disaster Monitoring, China University of Mining and Technology, Xuzhou, China. He has authored more than 50 peer-reviewed articles. His recent research interests include satellite navigation, inertial navigation and their integration and geodetic applications, and statistical estimation theory.

NANSHAN ZHENG was born in Anqing, China, in 1974. He received the B.Sc. and M.Sc. degrees in geodesy and surveying engineering from the China University of Mining and Technology, Xuzhou, China, in 1995 and 1998, respectively, and the Ph.D. degree in urban environment from Kyoto University, Japan, in 2009.

Since 2010, he has been with the School of Environmental Science and Spatial Informatics, China University of Mining and Technology, as a Professor, where he is currently the Vice Dean. He has authored or co-authored more than 60 peer-reviewed journal or conference articles. His recent research interests include GNSS-R, remote sensing, and risk assessment of environmental disasters.

TIANHE XU was born in Huanggang, China, in 1975. He received the B.Sc., M.Sc., and Ph.D. degrees in geodesy and surveying engineering from Information Engineering University, Zhengzhou, China, in 1998, 2001, and 2004, respectively.

He is with the Xi'an Institute of Surveying and Mapping, from 2001 to 2015. He was with GFZ as a Visiting Scientist, from 2009 to 2011. He has been with the State Key Laboratory of Geo-Information Engineering, Xi'an, China, since 2012, and also with the Institute of Space Sciences, Shandong University, Weihai, China, as a Professor, since 2016. He is also a Guest Professor with the School of Geological Engineering and Surveying and Mapping, Chang'an University, Xi'an. He has authored or co-authored more than 100 peer-reviewed journal or conference articles. His recent research interests include global navigation satellite systems' data processing and satellite gravimetry.

Dr. Xu was a recipient of the National Excellent Doctoral Dissertation Award, in 2007, and several other awards.